Integration and Evaluation of Forecast-Informed Multiobjective Reservoir Operations

Guang Yang[1]; Shenglian Guo[2]; Pan Liu[3]; and Paul Block, M.ASCE[4]

Abstract: Incorporating streamflow forecasts into reservoir operations can improve water resources management efficiency, yet the forecast value in multipurpose reservoir systems is rarely investigated, let alone the relationship between forecast accuracy and value in multiobjective reservoir operation. Here, we propose a forecast-informed framework to derive multiobjective operating rules based on radial basis functions and the Pareto archived dynamically dimensioned search optimization algorithm and subsequently develop indicators reflective of Pareto fronts with and without forecast information to characterize forecast value. Based on a case study of the Hanjiang cascade of reservoirs in the Yangtze River Basin, China, the optimal inclusion of streamflow forecasts notably improves the performance of multiobjective reservoir operations, mainly by significantly increasing the hydropower generation. The relationship between forecast accuracy and value is explored by comparing four accuracy indicators (Nash–Sutcliffe efficiency, mutual information, correlation coefficient, and Kullback–Leibler distance) and forecast value. The correlation coefficient is found to be the most suitable forecast indicator given its high correlation with forecast value and stability in the regression. For multiobjective forecast-informed reservoir systems, it is critical to understand and define the relationship between forecast accuracy and forecast value; if improvements in accuracy lead to steep gains in value, investing in further forecast model development may be warranted. **DOI: 10.1061/(ASCE)WR.1943-5452.0001229.** *© 2020 American Society of Civil Engineers.*

Author keywords: Reservoir operation; Radial basis functions; Forecast-informed reservoir operating rules; Forecast value; Multiobjective optimization.

Introduction

Rapid socioeconomic development and the subsequent increasing demand on water resources in many locations globally is challenging strategies to sufficiently supply water for things such as consumption, power generation, and ecosystem protection. Built infrastructure, namely, multipurpose reservoirs, remains one of the most common approaches to mitigate water scarcity and balance competing water interests. Developing an effective infrastructure management framework is equally critical and can lead to significant increases in benefits and cost savings (Bolouri-Yazdeli et al. 2014; Gleick and Palaniappan 2010; Labadie 2004; Stedinger et al. 1984; Yang et al. 2017b).

Seasonal and subseasonal streamflow forecasts provide a noninfrastructural management approach, given their recent significant advancements (Gibbs et al. 2018; Ismail and Bogacki 2017; Mortensen et al. 2018; Sene et al. 2018). In these studies, the accuracy and lead time in streamflow forecast are increased by using climate-index and error-correction techniques (such as data assimilation). For example, Gibbs et al. (2018) used a rainfall-runoff model with state updating and representative calibration-period selection to obtain monthly streamflow forecasts in southern Australia, with Nash–Sutcliffe efficiency (NSE) values greater than 0.75. Sene et al. (2018) obtained net inflow forecasts for Lake Malawi and Lake Victoria with lead times up to 4–5 months by using prior streamflow, rainfall, and climate indices. Skillful predictions from weeks to seasons are commonly applied to improve reservoir operation efficiency (Anghileri et al. 2016; Faber and Stedinger 2001; Sankarasubramanian et al. 2009) by explicitly incorporating forecasts into reservoir decision-making models using various techniques (Ficchì et al. 2015; Lu et al. 2017; Wang and Liu 2013; Yu et al. 2014). For example, Ficchì et al. (2015) integrated ensemble streamflow forecasts into operational models for four reservoirs in France using the model predictive control (MPC) method and demonstrated that the application of forecast information can significantly reduce flood control cost. Sankarasubramanian et al. (2009) optimized a reservoir operation model in conjunction with streamflow forecasts for the maximization of expected net revenue from water allocation. They found that streamflow forecasts can increase the annual yield and that forecast information is more valuable in water allocation systems with low storage-to-demand ratios.

In many cases, forecast-informed reservoir operations outperform traditional (static operations) approaches, with the added benefit defined as *forecast value*. In general—but not ubiquitously—more skillful streamflow forecasts are expected to lead to more effective decision-making and reservoir allocation strategies; however, improvement in forecast quality may not be linearly nor fully

[1]Ph.D. Researcher, School of Water Resources and Hydropower Engineering, Wuhan Univ., Wuhan, Hubei 430072, China; Postdoctoral Fellow, Dept. of Civil and Environmental Engineering, Univ. of Wisconsin-Madison, Madison, WI 53706. ORCID: https://orcid.org/0000-0001-7330-3502. Email: yang_guang@whu.edu.cn

[2]Professor, State Key Laboratory of Water Resources and Hydropower Engineering Science, Wuhan Univ., Wuhan, Hubei 430072, China; Professor, School of Water Resources and Hydropower Engineering, Wuhan Univ., Wuhan, Hubei 430072, China (corresponding author). Email: slguo@whu.edu.cn

[3]Professor, School of Water Resources and Hydropower Engineering, Wuhan Univ., Wuhan, Hubei 430072, China.

[4]Associate Professor, Dept. of Civil and Environmental Engineering, Univ. of Wisconsin-Madison, Madison, WI 53706.

Note. This manuscript was submitted on November 28, 2018; approved on January 13, 2020; published online on March 30, 2020. Discussion period open until August 30, 2020; separate discussions must be submitted for individual papers. This paper is part of the ***Journal of Water Resources Planning and Management***, © ASCE, ISSN 0733-9496.

J. Water Resour. Plann. Manage., 2020, 146(6): 04020038

translated into an increase in forecast value (Laio and Tamea 2007; Watkins and Wei 2008). This is partially attributable to reservoir specifics, including operational objectives, targets, and physical design (Boucher et al. 2012; Georgakakos 1989; Rosenberg et al. 2011). Numerous studies have investigated the relationship between forecast skill and value for different operating objectives such as hydropower generation (Alemu et al. 2010; Lamontagne and Stedinger 2018; Voisin et al. 2006) and water supply (Anghileri et al. 2016; Georgakakos et al. 2005; Sankarasubramanian et al. 2009; Turner et al. 2017). For example, Alemu et al. (2010) refined hydropower operating rules by using medium-range forecasts and concluded that the use of forecast information can significantly improve economic profits. Anghileri et al. (2016) developed a forecast-based adaptive management framework to guide the operation of water supply systems in snow-dominated river basins and evaluate the value of seasonal and interannual forecast data. Lamontagne and Stedinger (2018) generated synthetic streamflow forecasts with specific precision using the generalized maintenance of variance extension (GMOVE) method and applied it to a stochastic optimization model of a single reservoir hydropower system to illustrate how more skillful forecasts lead to improvements in system operations.

Few studies (Denaro et al. 2017; Turner et al. 2017) evaluated the forecast value for multiobjective reservoir systems. Turner et al. (2017) incorporated streamflow forecasts into a multipurpose reservoir system, focusing on the relationship between the forecast value and skill for a single-objective operation only (by considering target releases and target storage objectives separately.) For true multiobjective reservoir operations, there exists a trade-off among many different operating targets (Xu et al. 2015); an improvement gained for one target may only be achieved by making concessions to another target. This motivates the need for coincident consideration of numerous reservoir operation objectives when evaluating forecast value. Although Denaro et al. (2017) considered two reservoir operating targets (flood control and water supply) simultaneously in forecast value evaluation, until now, the relationship between multiobjective reservoir operation forecast value and forecast skill has never been investigated. Here, we propose a forecast-informed framework to derive multiobjective operating rules (MOOR) and use the forecast value indicator for multiobjective reservoir operation (Denaro et al. 2017) to search for the relationship with forecast accuracy. Specifically, we explore how forecast information affects the MOOR by addressing the following questions:

1. How can streamflow forecasts be incorporated into MOOR?
2. How does forecast information from MOOR improve the multiobjective reservoir operation?
3. What is the relationship between forecast skill and value in multiobjective reservoir operations?

The framework proposed here starts with generating streamflow forecasts by adding an error term (Georgakakos and Graham 2008; Maurer and Lettenmaier 2004; Sankarasubramanian et al. 2009), conditioned on a specified forecast accuracy (Yan et al. 2014). Next, MOOR are parameterized using radial basis functions (RBFs) (Buşoniu et al. 2011; Giuliani et al. 2014, 2015a) and subsequently optimized by applying the Pareto archived dynamically dimensioned search (PA-DDS; Asadzadeh and Tolson 2013) evolutionary algorithm. The process is repeated without forecast-informed streamflow to illustrate the expected forecast value of MOOR by comparing the Pareto fronts obtained from the optimization with and without forecast information. This final step includes describing the relationship between forecast accuracy and MOOR performance. We select a case study in the Yangtze River Basin to demonstrate the framework and provide quantitative assessment.

This work contributes to a framework integrating the forecast information into MOOR, an improved understanding of how streamflow forecast accuracy relates to systems requiring MOOR, and may further inform continued development of streamflow forecast products and methodologies for integrating with reservoir decision-making.

Study Area and Data

Hanjiang Cascade of Reservoirs and Operating Rules

The Hanjiang River, the largest tributary to the Yangtze River in China, has a basin area of approximately 159,000 km^2 and length of 1,570 km. The river originates in the southwestern part of the Shaanxi province, flows east across the southern part of that province, and merges with the Yangtze River at Wuhan, the provincial capital with more than 10 million inhabitants. The annual mean temperature is 15°C–16°C and annual precipitation varies from 700 to 1,800 mm, with 70%–80% of the total amount occurring in the wet season from May to October (Li et al. 2009). The Hanjiang cascade includes the Ankang and Danjiangkou multipurpose reservoirs (Fig. 1) with streamflow records extending back more than 30 years. The average annual natural runoff (1980–2010) to the Ankang reservoir and intervening basin between the Ankang and the Danjiangkou reservoirs is 17.80 and 17.24 billion m^3, respectively.

The Ankang reservoir, located in the upper reach of the Hanjiang River, has an active storage volume of 1.47 billion m^3 and serves as an important hydropower base in Shaanxi province in China. The reservoir is mainly used for hydroelectric power generation (installed capacity: 800 MW), with secondary objectives of flood control. The downstream Danjiangkou reservoir, with an active storage of 19.05 billion m^3, is in the middle reach of the Hanjiang River. The Danjiangkou controls 60% of the catchment area, serves as a key flood control project, and provides allocations for water supply and hydropower generation (installed capacity: 900 MW). The characteristic parameter values of the Ankang and Danjiangkou reservoirs are listed in Table 1.

In this study, the objective of flood control in the operation of the two reservoirs is to disallow exceeding prespecified water levels during the flood season (water level limits in Fig. 2), thus it can be translated into the constraints of the control problem. The Ankang reservoir mainly uses water releases for power generation (Chinese National Committee on Large Dams 2011) under some conventional constraints. As for the Danjiangkou reservoir, it primarily serves as a supply for the south-to-north water transfer project in China, and secondarily for power generation. Water supply releases of 135, 260, 300, 350, and 420 m^3/s are required based on reservoir water levels in Regions 1, 2, 3, 4, and 5, respectively (see operating rule curves in Fig. 2). For the south-to-north project, water is directly released from the reservoir through a special canal and thus is not available for power generation, while water releases for power generation can also be used to meet the discharge requirement downstream of the Danjiangkou reservoir (greater than 490 m^3/s) for navigation and ecosystem habitat. After meeting the discharge requirements, priorities are water supply and power generation, respectively (Sun et al. 2017; Yang et al. 2017a).

Data and Parameter Settings

Observed inflow (10-day average, 1980–2010) and other meteorological data (temperature, precipitation, etc.) are provided by the Changjiang Water Resources Commission of China. Reservoir characteristics data and basic reservoir operating rules are provided by the Hanjiang Group. Inflow to the Ankang reservoir and

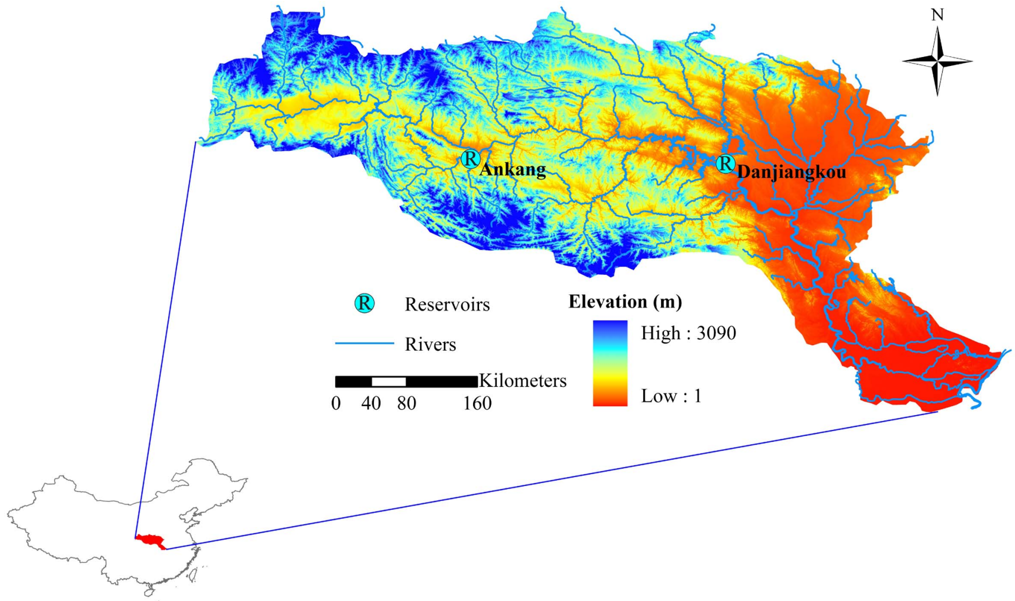

Fig. 1. Locations of the Hanjiang basin and cascade reservoirs.

Table 1. List of characteristic parameter values of the Ankang and Danjiangkou reservoirs

Reservoir	Unit	Danjiangkou	Ankang
Total storage	Billion m^3	33.04	3.20
Flood control storage in summer	Billion m^3	14.10	0.36
Flood control storage in autumn	Billion m^3	11.10	0.36
Crest elevation	m	176.6	338.0
Normal pool water level	m	170.0	330.0
Flood limited water level in summer	m	160.0	325.0
Flood limited water level in autumn	m	163.5	325.0
Dead water level	m	150.0	305.0
Fluctuating water level	m	145.0	300.0
Install capability	MW	900	800
Annual generation	Billion kW · h	3.8	2.8
Regulation ability	—	Multiyear	Annually

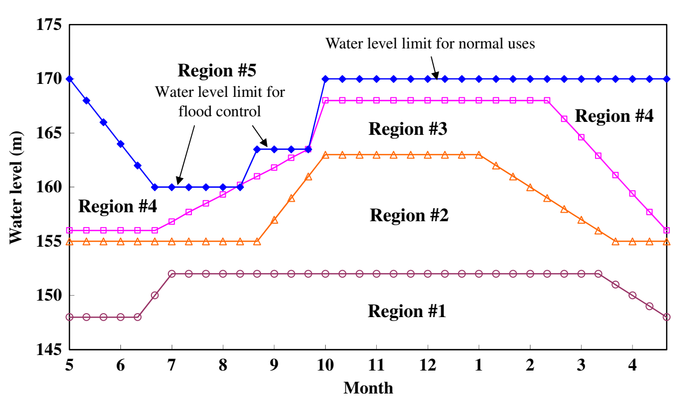

Fig. 2. Designed operation rule curves of the Danjiangkou reservoir.

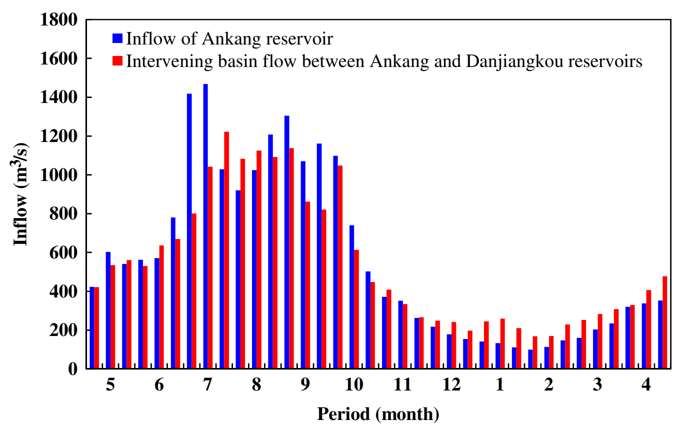

Fig. 3. The 10-day average inflow of Ankang reservoir and intervening basin flow between reservoirs during 1980–2010, respectively.

intervening basin flow between the Ankang and Danjiangkou reservoirs are expressed as $Q^{in}_{i-1,t}$ (m^3/s) and $Q^{inter}_{i,t}$ (m^3/s), respectively, illustrated in Fig. 3. The inflow to Danjiangkou reservoir is the sum of the outflow from the Ankang reservoir and the intervening basin flow, described in Eq. (4). The water year is defined as May to April.

In general, a longer lead time results in higher forecast values, given a certain forecast accuracy, for significantly large reservoirs. Many publicly available monthly datasets, such as climate hazards group infrared precipitation with station data (CHIRPS, Funk et al. 2015) and the Tropical Rainfall Measuring Mission's 3B43 (Huffman et al. 2007), provide high-resolution monthly global meteorological data which can serve as potential streamflow predictors; thus, a forecast lead time (time step) of one month (essentially three 10-day periods) is advantageous.

Methodology

The procedure for integrating forecasts and assessing forecast value in MOOR (Fig. 4) is introduced in this section.

- First, the general reservoir operating rules (without considering forecasts) described by the RBFs (of observed data) are

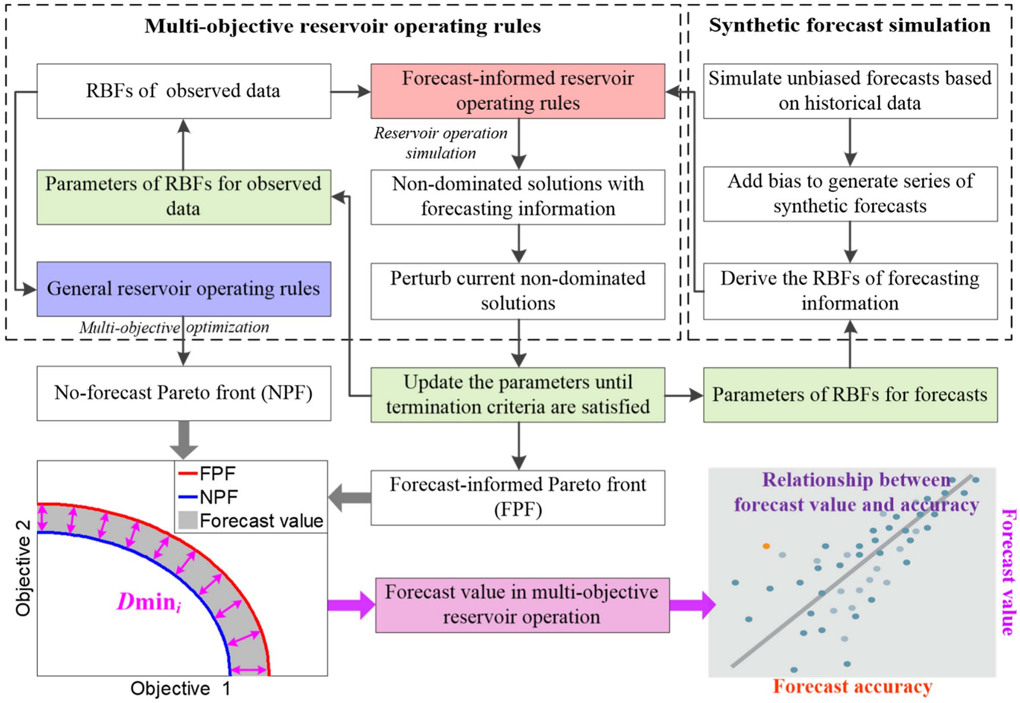

Fig. 4. Procedure for integrating the forecasts and assessing the forecast value in multiobjective reservoir operation.

optimized using the PA-DDS algorithm; the no-forecast Pareto front (NPF) is obtained after the multiobjective optimization.

- Second, synthetic forecasts with a specified accuracy and bias are generated from observed streamflow data (Yan et al. 2014) and used to derive the forecast-informed reservoir operating rules [Eq. (9)].
- Third, the forecast-informed reservoir operating rules are optimized using the PA-DDS algorithm, and the forecast-informed Pareto front (FPF) is obtained. In the multiobjective optimization, parameters for both the RBFs for observed data and RBFs for forecasts are updated until termination criteria are satisfied.
- Fourth, the forecast value in MOOR is evaluated by comparison of Pareto fronts from the optimal reservoir operating rules with and without forecast information. Higher forecast values occur for wider separation between Pareto fronts (Fig. 4, bottom left panel.) More details regarding forecast value are presented in the following sections.
- Finally, the relationship between forecast accuracy and value is evaluated by regressing forecast value against several forecast accuracy indicators. The most suitable forecast accuracy indicator is then selected to assess the forecast value of the multiobjective reservoir operation framework with a linear regression between the forecast accuracy and the forecast value (Fig. 4, bottom right panel.) The slope of the regression line represents the sensitivity of forecast value to accuracy.

Multiobjective Reservoirs Operation Model

Objective Equations

In addition to flood control, water supply and power generation are the most important reservoir functions. Thus, the objective functions can be expressed as the maximization of power generation and water supply for the reservoirs [Eqs. (1) and (2)]. The flood control (Fig. 2) and irrigation objectives are translated into water release constraints. The ranking between different objectives is not considered in this multiobjective reservoir operation model

$$\text{Max } W = \sum_{t=1}^{T} Q_t^W \cdot \Delta t \tag{1}$$

$$\text{Max } E = \sum_{i=1}^{N}\sum_{t=1}^{T} P_{i,t} \cdot \frac{\Delta t}{3600}, \qquad P_{i,t} = K_i \cdot Q_{i,t}^P \cdot H_{i,t} \tag{2}$$

where W and E = sum of the water supply (m^3) and energy generation ($kW \cdot h$), respectively; t = tth time period; i = ith reservoir; T = total number of operational periods; N = total number of reservoirs; Q_t^W (m^3/s) = water supply flow of the Danjiangkou reservoir in period t; (Δt) = amount of time during a single period; $P_{i,t}$ (kW) = power output of the ith reservoir in period t; K_i = hydropower generation efficiency of the ith reservoir; $Q_{i,t}^P$ (m^3/s) = water release for power generation of the ith reservoir in period t; and $H_{i,t}$ (m) = average hydropower head of the ith reservoir in period t. Only the downstream (Danjiangkou) reservoir is used for the water supply, which is controlled by the established operating rule curves (Fig. 2) and is withdrawn directly from the reservoir for the south-to-north water transfer project in China.

Equations and Constraints

Water Balance. The reservoir water balance describing the change in storage is as follows:

$$S_{i,t+1} = S_{i,t} + (Q_{i,t}^{in} - Q_{i,t}^{out}) \cdot \Delta t' - ES_{i,t} \tag{3}$$

where $S_{i,t}$ (m^3) and $S_{i,t+1}$ (m^3) = storage of the ith reservoir in period t and $t+1$, respectively; $Q_{i,t}^{in}$ (m^3/s) and $Q_{i,t}^{out}$ (m^3/s) = inflow and total water release of the ith reservoir in period t, respectively; $\Delta t'$ (s) = time step (10 days in this study); and $ES_{i,t}$ (m^3) = sum of evaporation and seepage from the ith reservoir in period t. For situations in which the water supply is withdrawn directly from the reservoir, the Danjiangkou reservoir total release consists of the water used for water supply and power generation.

Reservoir Inflow. The inflow of the Ankang reservoir is the aforementioned $Q_{i-1,t}^{in}$ (Fig. 3), and the inflow into the Danjiangkou reservoir can be expressed as

$$Q_{i,t}^{in} = Q_{i-1,t}^{out} + Q_{i,t}^{inter} \quad (4)$$

where $Q_{i-1,t}^{out}$ (m^3/s), $Q_{i,t}^{inter}$ (m^3/s), and $Q_{i,t}^{in}$ (m^3/s) = outflow from the Ankang reservoir, intervening tributary and overland flow between the Ankang and Danjiangkou reservoirs, and inflow into the Danjiangkou reservoir in period t, respectively.

Reservoir Storage. The physical constraints of the reservoirs can be expressed as

$$S_{i,t}^{\min} \le S_{i,t} \le S_{i,t}^{\max} \quad (5)$$

where $S_{i,t}^{\min}$ (m^3) and $S_{i,t}^{\max}$ (m^3) = minimum and maximum water storage of the ith reservoir in period t, respectively.

Reservoir Releases. Reservoir releases are contingent on downstream demands, specifically

$$Q_{i,t}^{\min} \le Q_{i,t}^{out} \le Q_{i,t}^{\max} \quad (6)$$

where $Q_{i,t}^{\min}$ (m^3/s) and $Q_{i,t}^{\max}$ (m^3/s) = minimum and maximum releases of the ith reservoir in period t for all downstream uses, respectively, which are determined by the downstream discharge requirement.

Power Generation Limits.

$$P_{i,t}^{\min} \le P_{i,t} \le P_{i,t}^{\max} \quad (7)$$

where $P_{i,t}^{\min}$ (kW) and $P_{i,t}^{\max}$ (kW) = minimum and maximum power generation of the ith reservoir in period t, which are determined based on the installed capacity and turbines features.

Mass Conservation.

$$S_{i,t} = \begin{cases} S_i^{begin} & t = 1 \\ S_i^{end} & t = T \end{cases} \quad (8)$$

where S_i^{begin} (m^3) and S_i^{end} (m^3) = beginning and ending storage in the ith reservoir at the start and completion of each simulation, respectively. The storage of each reservoir at the end of the simulation time horizon is equivalent to the storage at the beginning of the simulation in this study. This constraint is included to ensure water is retained in the reservoir for future operations. If excluded, the model will empty the reservoir by the end of the simulation horizon to maximize water supply or power generation artificially.

Forecast-Informed Operating Rules

To determine the total water release for each reservoir, we use the RBF model to integrate available information into reservoir operating rules. The information used in the RBFs here includes observed data (e.g., reservoir inflow and storage) in the current period and forecasted data. For each reservoir, we select the corresponding reservoir storage, inflow, and seasonal information τ_t [where τ_t refers to the position of the current period t within a water year, e.g., it equals 1 when t is $1(36\times 0+1)$, $37(36\times 1+1), 73(36\times 2+1)\ldots$, considering that there are 36 periods within a water year] in the current period as observed input variables, and select the average streamflow forecast across the next month (i.e., the forecast lead time is 1 month) as forecasted input variables in this study. The decision time step in the reservoir operation is 10 days and the optimization horizon is 31 years (1980–2010,) i.e., there are 1116 (31×36) time steps in the optimization horizon.

The Gaussian RBF model is demonstrated to possess strong mathematical properties of universal approximation (Tikk et al. 2003), thus the adoption of the universal approximator (Gaussian RBF) can ensure flexibility to the structure of the operating rules [for more applications of the RBF model in reservoir operation see Deisenroth et al. (2013) and Giuliani et al. (2014, 2015a)]. Therefore, the forecast-informed reservoir operating rules are defined with Gaussian RBFs by the following equations:

$$Q_t^{out} = \sum_{u=1}^{U} \omega_u \varphi_u(X_t) + \sum_{f=1}^{F} \omega_f \varphi_f(Y_t), \quad t = 1, \ldots, T \quad (9)$$

$$\varphi_u(X_t) = \exp\left\{-\frac{1}{b_u^2}\sum_{j=1}^{M}[(X_t)_j - c_{j,u}]^2\right\} \quad c_{j,u}\in[-1,1], \quad b_u\in(0,1] \quad (10)$$

$$\varphi_f(Y_t) = \exp\left\{-\frac{1}{b_f^2}\sum_{j=1}^{L}[(Y_t)_j - c_{j,f}]^2\right\} \quad c_{j,f}[-1,1], \quad b_f\in(0,1] \quad (11)$$

where Q_t^{out} (m^3/s) = reservoir water release in period t; $\varphi_u(\cdot)$ and $\varphi_f(\cdot)$ = RBFs using the observed and forecasted data, respectively; U and F = total number of RBFs and ω_u and ω_f = RBF weights for the observed and forecasted data, respectively; M and L = total number of observed input variables X_t and forecasted input variables Y_t, respectively; and c_j and b = center and radius of the RBFs, respectively.

If $\sum_{f=1}^{F}\omega_f\varphi_f(Y_t)$ in Eq. (9) is not included [i.e., $Q_t^{out} = \sum_{u=1}^{U}\omega_u\varphi_u(X_t)$], the equation collapses to the general (no-forecast-informed) reservoir operating rules. To fully express the reservoir operating policies, the number of RBFs describing the reservoir operating rules is determined through a sensitivity analysis, i.e., increasing the RBFs until the benefits of optimal solutions do not change significantly. Ultimately, the number of RBFs for observed and forecasted flow data in the MOOR are set as four [as in Yang et al. (2017b)] and three, respectively. Thus for each reservoir, $M = 3$ (the three variables are reservoir storage, inflow, and seasonal information τ_t), $U = 4$, $F = 3$, and $L = 1$ (for Ankang: the average forecast of reservoir inflow; for Danjiangkou: the intervening flow between the Ankang and Danjiangkou reservoirs across the next month) in Eqs. (9)–(11); there are 20 and 9 parameters to be calibrated for the sum of RBFs for the observed and forecasted data, respectively. Therefore, for the cascade reservoir operation, there are $40(20\times 2)$ and $58[(20\times 2)+(9\times 2)]$ parameters in general and forecast-informed reservoir operating rules, respectively.

We optimize these parameters based on a simulation-optimization model (Rani and Moreira 2010) using the PA-DDS evolutionary algorithm as previously applied to water resources management (Yang et al. 2017a). To produce the Pareto front, the PA-DDS algorithm adopts the Pareto archived evolution strategy, where its simplest form uses a local and single-solution-based optimization strategy to explore the search space and archives all the nondominated solutions during the search procedure (Knowles and Corne 1999). The procedure of the PA-DDS algorithm has been described in detail by Asadzadeh and Tolson (2013) and is described in the following steps:

1. Initialize the starting solutions by using the DDS algorithm (Tolson and Shoemaker 2007) to maximize each objective

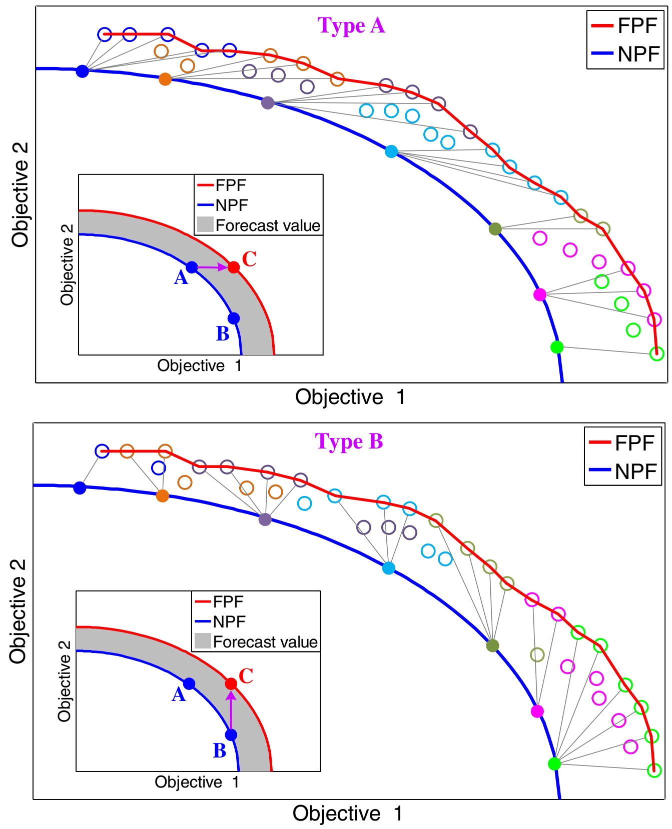

Fig. 5. Pareto fronts illustrating the direction in improvement of reservoir operations when conditioned with forecast information. For the seven points (solid circle) on the NPF, each subsequently produces multiple corresponding points (open circle) to form the FPF. Points A and B denote outcomes from the no-forecast rules; point C denotes the outcome condition on forecast-informed rules. Two directions of improvement are possible (Types A and B) by increasing either Objective 1 or 2.

(water supply and power generation) and randomly generating solutions between the bounds.

2. Calculate the crowding distance (which is described by the average distance of two neighboring solutions) of solutions in the external set and select a nondominated solution based on crowding distance.
3. Generate new solutions by perturbing the randomly selected decision variables of the current solution with a probability which decreases as the number of iterations (from Step 1 to Step 5) increase from one to the maximum number of function evaluations.
4. Check the dominance of the newly generated solutions against the external set of solutions. If the new solution is nondominated, the current solution is updated with the new solution; otherwise, a new current solution is selected from the external set of the nondominated solutions. For no-forecast and forecast-informed rules, the parameters in $\sum_{u=1}^{U}\omega_u\varphi_u(X_t)$ and $\sum_{u=1}^{U}\omega_u\varphi_u(X_t)+\sum_{f=1}^{F}\omega_f\varphi_f(Y_t)$ are updated, respectively. As illustrated in Fig. 4, only the parameters of RBFs for observations are updated to produce the NPF; however, the parameters of RBFs for both observations and forecasts are updated to produce the FPF.
5. Repeat Steps 2–4 until the maximum number of function evaluations is exceeded. The number can be user-defined before the optimization according to the complexity of the problem.

There are two parameters in the PA-DDS optimization algorithm: the neighborhood perturbation size parameter (r) and the maximum of the function evaluation. Given the relative insensitivity of the multiobjective optimization performance to parameter settings in the PA-DDS algorithm, r is set to its default value (0.2) (Asadzadeh and Tolson 2009) and the maximum of the function evaluation is set to 50,000.

To investigate potential improvement in reservoir operations when including forecast information, we optimize the RBFs for the observed data first and subsequently the RBFs for the forecasted data, in lieu of optimizing the RBFs simultaneously. In this way, each point on the NPF will produce a Pareto front, and the FPF may be constructed by combining all Pareto fronts (Fig. 5). Two directions from NPF to FPF are possible (Fig. 5) for the two-objective optimization problem, and the direction of improvement conditioned on forecasts may vary even for the same NPF and FPF.

Forecast Streamflow Simulation

A Monte Carlo approach is used to generate synthetic streamflow forecast series with a specified accuracy, based on historical streamflow data. It is assumed that the relative forecast error ε_t at each time period is approximately normally distributed (Stedinger et al. 2008). The NSE (Nash 1970) is selected as an indicator of streamflow forecast precision. The general procedure is presented here; for additional details readers are encouraged to review Yan et al. (2014).

NSE is mathematically represented by the equation

$$\mathrm{NSE} = 1 - \frac{\sum_{t=1}^{T}(y_t' - y_t)^2}{\sum_{t=1}^{T}(y_t - \bar{y})^2} \tag{12}$$

where y_t' and y_t = forecast and observed streamflow in time period t, respectively; $\bar{y}$ = mean of the observed streamflow; and T = total number of streamflow data time periods.

Eq. (12) can be expressed by

$$\sum_{t=1}^{T}(y_t - \bar{y})^2(1-\mathrm{NSE}) = \sum_{t=1}^{T}(y_t' - y_t)^2 = \sum_{t=1}^{T}(\varepsilon_t^2 y_t^2) \tag{13}$$

where $\varepsilon_t = (y_t' - y_t)/y_t$ = relative forecast error.

Suppose that the relative error is unbiased and normally distributed, $\varepsilon_t \sim N(0, \sigma_\varepsilon^2)$, where σ_ε is related to forecast accuracy (i.e., smaller values of σ_ε correspond with more accurate forecasts), then the expected value of the relative forecast error can be obtained by $E(\varepsilon_t^2) = Var(\varepsilon_t) + E^2(\varepsilon_t) = \sigma_\varepsilon^2$.

The expected value of the left side of Eq. (13) can be expressed as

$$E\left[\sum_{t=1}^{T}(y_t - \bar{y})^2(1-\mathrm{NSE})\right] = \sum_{t=1}^{T}(y_t - \bar{y})^2(1-\mathrm{NSE}) \tag{14}$$

where $E[x]$ = expected value of x.

The expected value of the right side of Eq. (13) can be expressed as

$$E\left[\sum_{t=1}^{T}(\varepsilon_t^2 y_t^2)\right] = \sum_{t=1}^{T}[E(\varepsilon_t^2)y_t^2] = \sigma_\varepsilon^2\sum_{t=1}^{T}y_t^2 \tag{15}$$

According to Eq. (13), $\sum_{t=1}^{T}(y_t - \bar{y})^2(1-\mathrm{NSE})$ should be equal to $\sigma_\varepsilon^2\sum_{t=1}^{T}y_t^2$, thus the variance σ_ε^2 can be calculated by

$$\sigma_\varepsilon^2 = \frac{\sum_{t=1}^{T}(y_t - \bar{y})^2(1 - \mathrm{NSE})}{\sum_{t=1}^{n} y_t^2} \tag{16}$$

Finally, the streamflow forecast series can be simulated using

$$y_t' = y_t + \varepsilon_t y_t \tag{17}$$

Synthetic unbiased streamflow forecasts are generated by varying NSE. To systematically add potential forecast bias across flow conditions, streamflow categories (dry, normal, and wet) are selected based on observations within the ranges of percentile (0, 0.1), (0.1, 0.9), and (0.9, 1.0), respectively, and a bias representing underestimation and overestimation of observed streamflow by 10% and 20% is imposed. For instance, $\mathrm{Wet}_{\mathrm{p}20\%}$ implies there is a 20% (positive) increase for forecast values falling in the wet range, i.e., $y_t' = (y_t + \varepsilon_t y_t) \times 1.2$; $\mathrm{Dry}_{\mathrm{m}10\%}$ is a 10% (negative) reduction for forecast values falling in the dry category.

Indicators of Forecast Accuracy and Value

Three indicators (in addition to NSE as utilized above) are introduced to assess streamflow forecast performance: mutual information (Cover 1991), correlation coefficient, and Kullback–Leibler distance (KLD) (Kullback and Leibler 1951). The definition of these indicators is described below.

Mutual information (MI) is a widely used measure to define dependency between variables. Given two random variables x and y, their MI is defined in terms of their probabilistic density functions $p(x)$, $p(y)$, and $p(x,y)$ as below:

$$\mathrm{MI}(X;Y) = \sum_{y \in Y}\sum_{x \in X} p(x,y)\log\left[\frac{p(x,y)}{p(x)p(y)}\right] \tag{18}$$

Correlation coefficients (CC) quantify the strength of linear relationships between variables, ranging from −1 (perfect negative relationship) to 0 (no relationship) to 1 (perfect positive relationship):

$$\mathrm{CC} = \frac{Cov(x,y)}{\sqrt{Var(x)Var(y)}} \quad \rho_{x,y} \in [-1, 1] \tag{19}$$

KLD is a measure of how two probability distributions diverge from one another. Given two random variables x and y, KLD is defined in terms of their probabilistic density functions $p(x)$ and $p(y)$ as below:

$$\mathrm{KLD}(X;Y) = \sum_{y \in Y}\sum_{x \in X} p(x)\log\left[\frac{p(x)}{p(y)}\right] \tag{20}$$

The goal of this work is not to assess simply the streamflow forecast performance but rather the forecast value of reservoir operations resulting from a specified performance. For single-objective reservoir operation, the forecast value can be expressed by comparing objectives (e.g., power generation) with and without using forecast information. Forecast values for MOOR systems are more complicated, however, given the trade-offs between different targets (e.g., power generation and water supply). To address this, we use the difference in Pareto fronts resulting from the forecast and no-forecast approaches (represented as the width of the separation between Pareto fronts in Fig. 4, bottom left panel) to describe the MOOR forecast value. Given a specific no-forecast point P_i (the ith point in the NPF), the closest point in the FPF can be found. We calculate the Euclidean distance between the two points ($D\min_i$) for all points in the NPF and use their average value as the forecast value. This Euclidean-distance-based matrix has been introduced and used by Giuliani et al. (2015b) and Denaro et al. (2017) in multiobjective reservoir operation.

Given different objective types and units of measure, the objectives are normalized before the calculation of forecast value to minimize possible biases. For example, both power generation and water supply in this study are translated into economic profits, specifically, 0.21 Yuan RMB per kW · h (the electricity price for the Hanjiang cascade reservoirs) for hydropower and 0.13 Yuan RMB per m^3 (the water price) for water transfers in the south-to-north project, as in Yang et al. (2017b). Because the Euclidean-distance-based forecast value indicator calculates the shortest Euclidean distance ($D\min_i$) between the NPFs and FPFs, the forecast value here can be explained as the minimum monetary profit which can be obtained by using forecast-informed rules on average.

Results and Discussion

Multiobjective Reservoir Operation with Forecasted Flow Data

By varying the NSE value [from 0.40, 0.45, 0.50, ..., 0.95; 12 series; Eq. (17)], the forecast of the Ankang reservoir inflow and tributary flow between the Ankang and Danjiangkou reservoirs are simulated for Hanjiang cascade operations. Some comparisons of observed and forecasted streamflow are illustrated in Appendix S1 in the Supplemental Data. Considering that the same NSE can be achieved with very different forecasts, we repeat the generation of synthetic forecast for each NSE value and bias five times. The accuracy indicators (bias, NSE, CC, MI, and KLD) are calculated and their empirical frequency distributions are plotted in Fig. 6 as histograms. Clearly, the frequency or percentage of unbiased forecast series is higher than that of biased series. For normal streamflow, the percentage of unbiased (bias <5%) series in all the simulations is about 50%. The percentage of biased forecasts decrease with the degree of the bias, which is generally less than 20%. In contrast to the unevenly distributed MI and KLD values, NSE and CC are more evenly distributed (0.45–0.95 and 0.8–0.98, respectively).

The no-forecast and forecast-informed multiobjective optimization-based Pareto fronts for the Hanjiang cascade are initially compared for the unbiased forecasts across NSE values (Fig. 7). As NSE increases, the FPF moves in the direction of more power generation and water supply. To minimize the effects of the RBFs (RBFs for forecast-informed operating rules provide more flexibility than those for no-forecast reservoir operating rules), the results of reservoir operating rules with the worst forecast (NSE = 0) are also considered and found similar to the results of no-forecast multiobjective optimization. Recall from Eq. (12) that when NSE = 0, the mean value of the streamflow is used for the forecast.

Impact of Forecasts on Multiobjective Reservoir Operation

The directions of improvement in multiobjective Hanjiang cascade reservoirs operation caused by forecast information are shown in Fig. 8 with NPFs and FPFs. Most lines connecting the no-forecast and forecast-informed solutions in Fig. 8 are approximately parallel to the x-axis, which indicates that forecasts tend to improve the reservoir operation mainly by increasing the power generation. For the multiobjective system, the forecast-informed reservoir operation rules lead to more energy generation (additional 100 million kW · h per year) than those for no-forecast reservoir operating rules (Fig. 7). Thus, for this case study, forecast

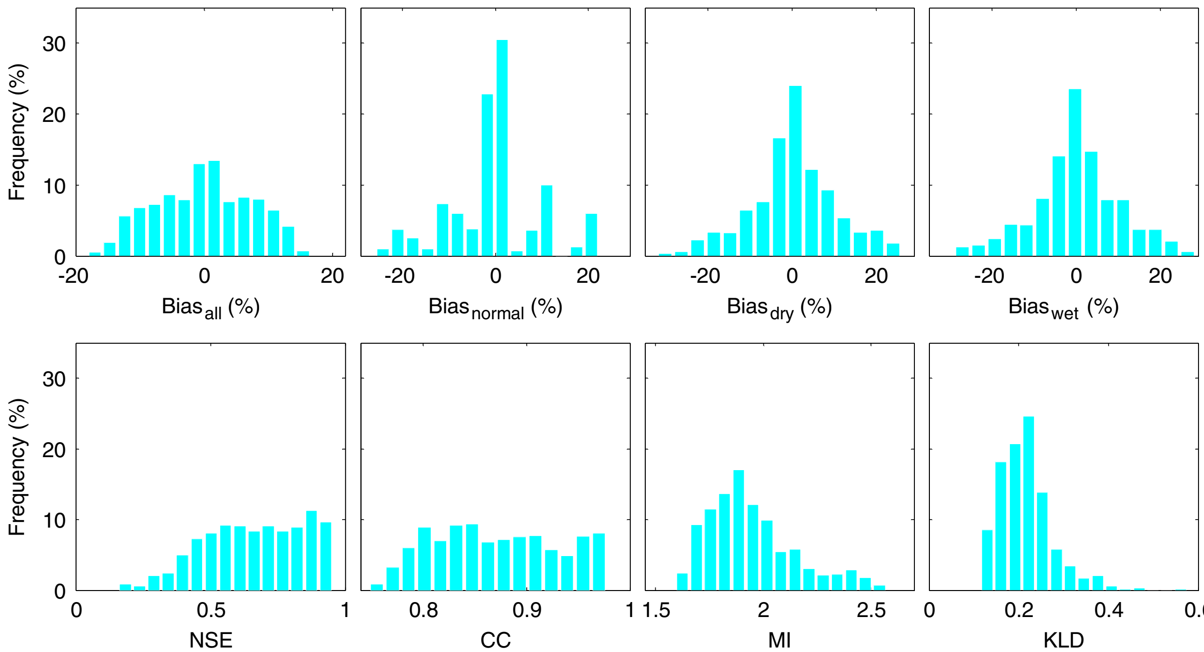

Fig. 6. Empirical frequency of accuracy indicators (bias, NSE, CC, MI, and KLD) of synthetic forecasts. The top and bottom panels describe the distribution of the bias and accuracy, respectively.

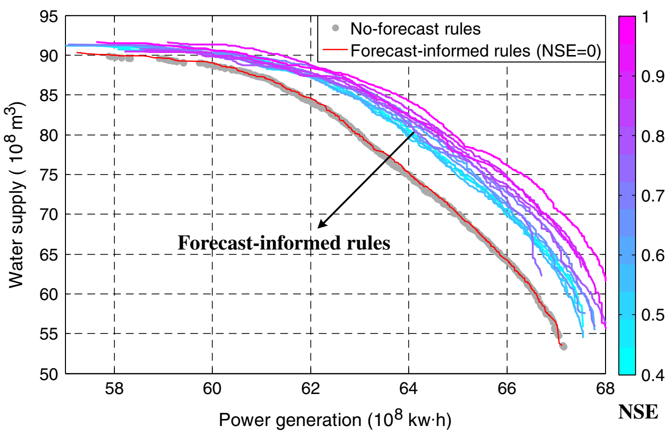

Fig. 7. Multiobjective optimization results of no-forecast and forecast-informed operating rules for Hanjiang cascade reservoirs. As the values of the NSE between the forecasted and observed flow data increases, the Pareto fronts of the forecast-incorporated rules moves to the region with additional power generation and water supply.

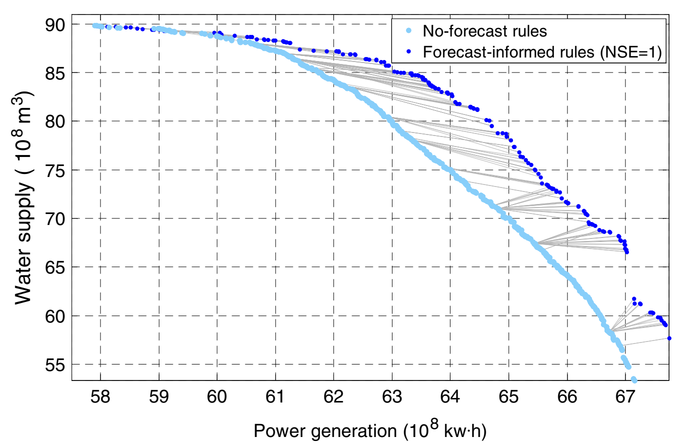

Fig. 8. Directions of improvement in multiobjective reservoirs operation caused by forecast information. The larger and smaller points refer to Pareto fronts obtained from no-forecast and forecast-informed rules, respectively, and each forecast-informed rule relates to one no-forecast solution, expressed with a line connecting the two points.

information appears to have a more significant impact on power generation than water supply, which is consistent with the findings in Turner et al. (2017).

One reason is that water supply is mainly controlled by water supply rule curves, which limits the impact of forecasts. Because water supply is determined by the reservoir water level and remains the same value within the same region (there are five regions in total; Fig. 2), water supply is not overly sensitive to reservoir releases and thus is not easily affected by forecasts. For example, the boundaries defining Region 2 from October to December are so wide (Fig. 2) that a change in water release conditioned on forecast information may not be sufficient to move the reservoir water level out of Region 2, thus not triggering a change in water supply during the time period. Another reason is that the value of the seasonal streamflow forecast tends to increase with a decrease in the capacity-inflow ratio (ratio of active reservoir capacity to annual reservoir inflow volume) (Anghileri et al. 2016). Thus, the Ankang reservoir (capacity-inflow ratio $= 0.082$), primarily utilized for power generation, may be more significantly influenced by forecasts than the Danjiangkou reservoir (capacity-inflow ratio $= 0.541$.)

The no-forecast rules and forecast-informed rules (using the forecast with NSE = 1) are optimized for power generation, and the corresponding annual mean reservoir water levels are compared with the perfect trajectory (the optimal reservoir water release in each time step across the full time horizon) optimized with dynamic

J. Water Resour. Plann. Manage., 2020, 146(6): 04020038

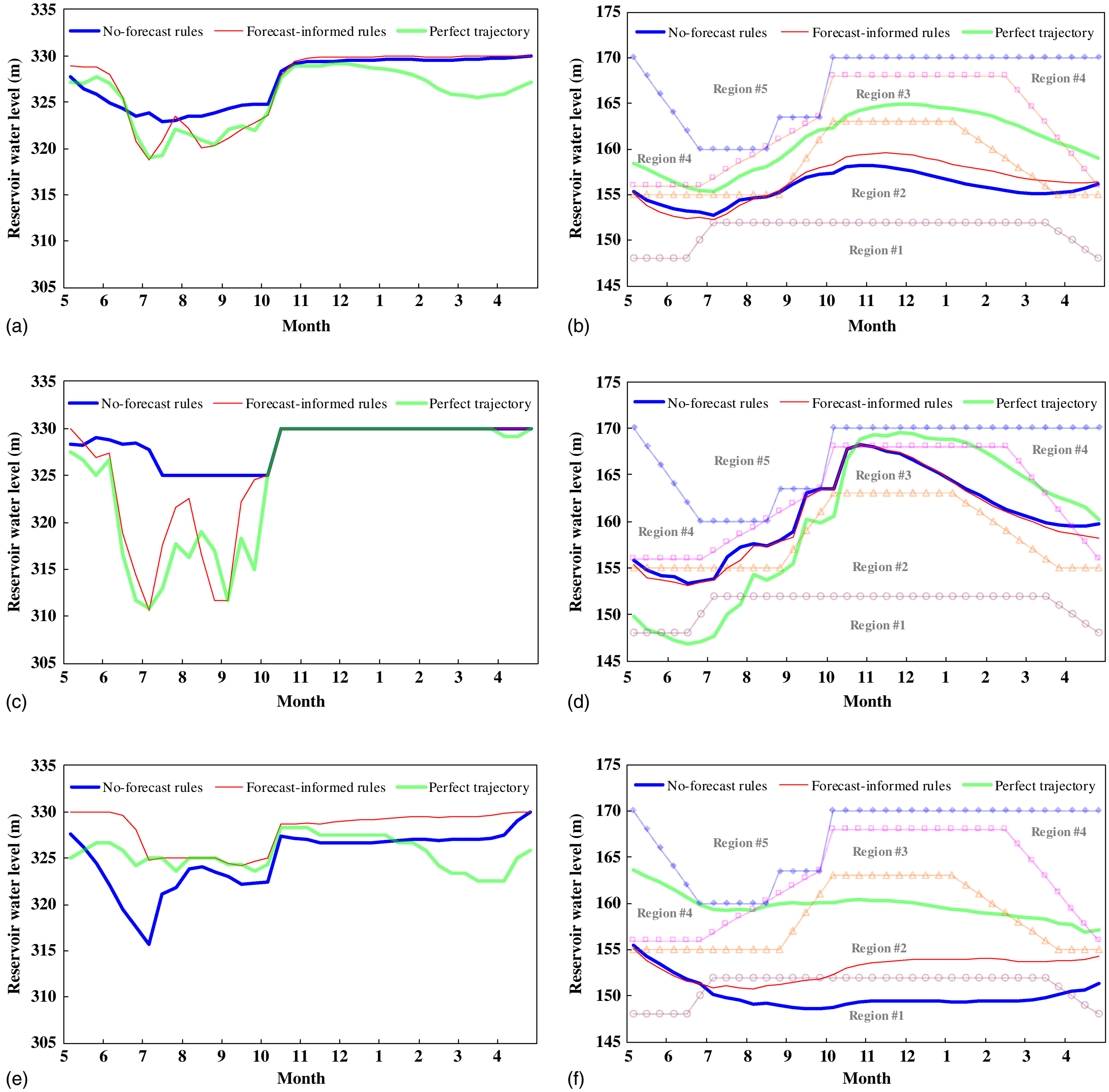

Fig. 9. Trajectories simulated by using general and forecast-informed reservoir operating rules for power generation for: (a) Ankang (all years); (b) Danjiangkou (all years); (c) Ankang (wet years); (d) Danjiangkou (wet years); (e) Ankang (dry years); and (f) Danjiangkou (dry years). Dry and wet years are represented as observed streamflow within the range of (0, 0.1) and (0.9, 1.0) quantiles, respectively.

programming (Fig. 9). It is evident that forecast-informed rules give the water levels of the Ankang and Danjiangkou reservoirs a closer-to-perfect trajectory than the no-forecast rules, which highlights the value of forecast information. Specifically, the forecast-informed rules force the Ankang reservoir water level to be lower during the flood season than the no-forecast rules do, which increases the power generation of the Hanjiang cascade. Compared with the no-forecast rules, the forecast-informed rules tend to keep lower and higher water levels for the Ankang and Danjiangkou reservoirs, respectively, in wet years, but the other way around in dry years.

Forecast Value in Multiobjective Reservoir Operation

Using the observed data and synthetically generated forecasts, the forecast accuracy metrics (NSE, CC, MI, and KLD) can be calculated with Eqs. (12), and (18)–(20). A strong correlation exists between forecast accuracy and value, as evidenced by the increase in forecast value with increasing NSE, CC, and MI and decreasing KLD (Fig. 10). The coefficient of determination (r^2) between the forecast value and NSE and CC is greater than between the forecast value and MI and KLD, indicating a stronger relationship with forecast value. Strikingly different outcomes between unbiased and

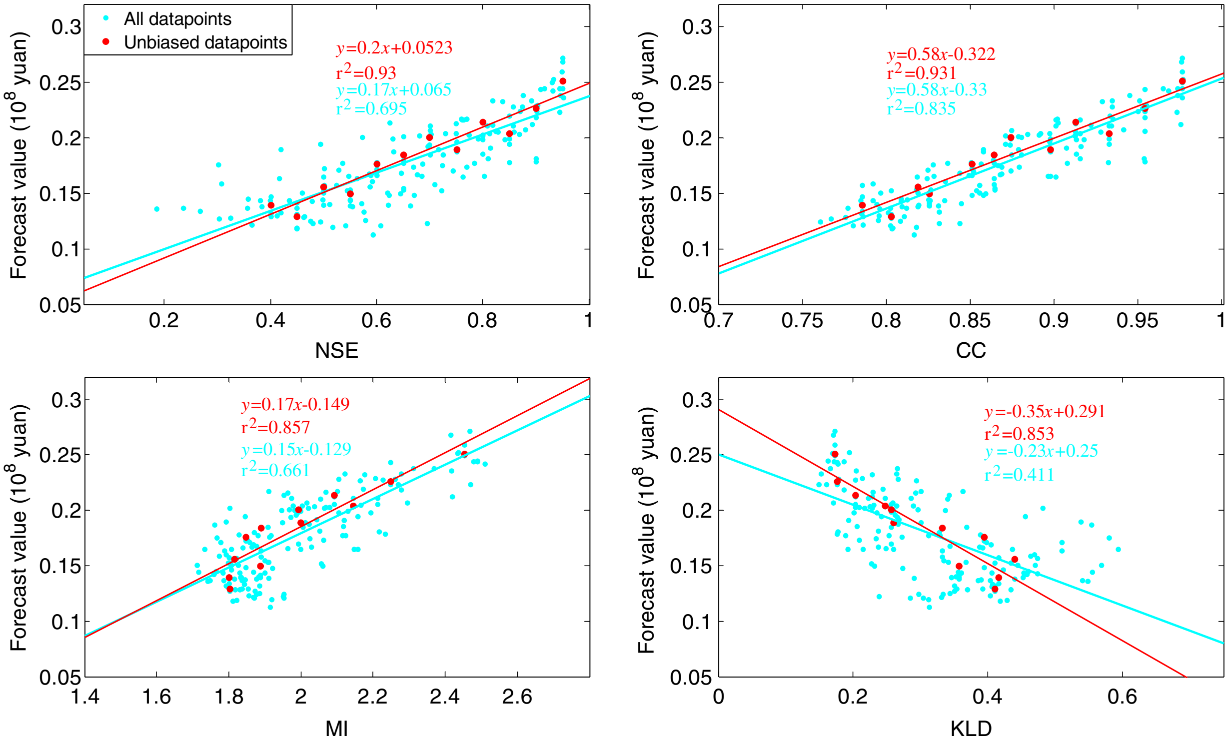

Fig. 10. Regression results between the forecast value and accuracy indicators (NSE, CC, MI, and KLD) in Hanjiang cascade reservoir operations. r^2 refers to the coefficient of determination in the regression; the data obtained from unbiased forecasts and all (including biased and unbiased) forecasts are regressed separately. If the two regression lines are similar to each other, the relationship between the forecast value and accuracy indicator is assumed to be robust and resistant to bias in the forecasts.

biased forecasts make it difficult to identify a stable relationship between forecast accuracy and value, especially when the information about forecast bias is unavailable.

As shown in the top panels of Fig. 6, the bias in synthetic streamflow forecasts can be as high as 20%, which decentriliazes the points, resulting in r^2 values lower than unbiased datapoints and even altering the regression line in Fig. 10. The regression line alteration is obvious in KLD (with the most significant difference both in slope and in intercept between the regression with all datapoints and unbiased datapoints) but barely noticeable in CC. The polynominal regression results between forecast accuracy indicators and forecast value (Table 2) also illustrate the impact of a biased forecast on r^2. Although the NSE and CC result in very high r^2 values for an unbiased forecast, only the CC always demonstrates an r^2 value greater than 0.8 when biased forecasts are included in the regression. Thus, from the aspects of precision and stability, the CC is the best indicator to evaluate the impact of forecasts on reservoir operation. Overall, the value of including forecasts in multiobjective operations for the Hanjiang cascade reservoirs results in approximatley 10 million and 20 million Yuan annually when the CC is 0.75 and 0.90, respectively (Fig. 10).

For the biased forecast, the NSE is a measure of precision that does not capture the systematic error (Lamontagne and Stedinger 2018), which means that the NSE treats the bias (or systematic error) as the forecast error. However, the systematic error caused by bias is different from the forecast error because it can be significantly corrected by statistical methods. Compared with the CC, which can capture both the precision and systematic error, the NSE tends to overestimate the forecast error if the systematic error can be corrected.

Table 2. Coefficient of determination (r^2) for the polynomial regression between four forecast accuracy indicators and forecast values for unbiased and all (biased + unbiased) data points

Data points	Unbiased data points			All data points		
Degree of polynomial	One	Two	Three	One	Two	Three
NSE	0.930	0.931	0.933	0.695	0.749	0.749
CC	0.931	0.931	0.935	0.835	0.838	0.838
MI	0.857	0.891	0.908	0.661	0.661	0.669
KLD	0.853	0.869	0.869	0.411	0.542	0.542

Conclusions

The application of streamflow forecasts can improve reservoir operation efficiency considering multiple targets; however, forecast value in multipurpose reservoir systems is rarely investigated, especially in terms of its relationship with forecast skill. This work explicitly incorporates streamflow forecasts into reservoir operating rules to explore the impact of forecast information on multiobjective reservoir operations.

Using the Hanjiang cascade reservoirs in the Yangtze River Basin, China, we propose a forecast-informed framework to derive MOOR, evaluate the forecast value in MOOR by comparing Pareto fronts of the no-forecast and forecast-informed rules, and search for the relationship between forecast value and forecast skill by evaluating synthetic streamflow forecasts with varying skill. The main conclusions of this study are summarized as follows:

1. The proposed forecast-informed reservoir operating rules can notably improve the performance of multiobjective reservoir operations; implementing forecast-informed rules could increase

power generation by 100 million kW · h per year for the Hanjiang system.
2. Streamflow forecasts tend to improve Hanjiang reservoir operations predominantly by increasing hydropower generation; the Ankang reservoir (small capacity-inflow ratio) is more sensitive to forecast information than the Danjiangkou reservoir (large capacity-inflow ratio.)
3. A linear relationship between forecast skill and value in multiobjective reservoir operations is evident; the correlation coefficient (CC) between observed and forecasted flow is less influenced by forecast bias in the relationship between forecast accuracy and forecast value than other candidate forecast accuracy indicators.

In summary, we have answered the three questions posed in the introduction regarding how forecast information affects the MOOR: (1) streamflow forecasts can be effectively incorporated into MOOR by combining RBFs from both observed and forecast data; (2) forecast information can improve multiple reservoir operating objectives simultaneously; however, improvement varies with the objective selected, specifically, power generation is more sensitive to streamflow forecast information than water supply for this case study; and (3) forecast value in multiobjective reservoir operations increases with forecast skill, and the strength and stability of their relationship highly depends on the indicator describing the streamflow forecast skill.

These findings can inform the expected value of integrating forecasts into MOOR and potential additional benefits resulting from further improvements in forecast model accuracy. This work is primarily focused on evaluating the impacts of forecast quality and operation objectives on forecast value, although reservoir characteristics may also be an important determinant. Further work could consider the synergistic effects of both forecast flow and reservoir characteristics to better gauge expected forecast value.

Data Availability Statement

The data used in this paper can be requested by contacting the corresponding author.

Acknowledgments

This study was financially supported by the National Natural Science Foundation of China (Grant Nos. 51539009 and 51879192).

Supplemental Data

Appendix S1 and Figs. S1 and S2 are available online in the ASCE Library (www.ascelibrary.org).

References

Alemu, E. T., R. N. Palmer, A. Polebitski, and B. Meaker. 2010. "Decision support system for optimizing reservoir operations using ensemble streamflow predictions." *J. Water Resour. Plann. Manage.* 137 (1): 72–82. https://doi.org/10.1061/(ASCE)WR.1943-5452.0000088.

Anghileri, D., N. Voisin, A. Castelletti, F. Pianosi, B. Nijssen, and D. P. Lettenmaier. 2016. "Value of long-term streamflow forecasts to reservoir operations for water supply in snow-dominated river catchments." *Water Resour. Res.* 52 (6): 4209–4225. https://doi.org/10.1002/2015WR017864.

Asadzadeh, M., and B. A. Tolson. 2009. "A new multi-objective algorithm, Pareto archived DDS." In *Proc., 11th Annual Conf. Companion on Genetic and Evolutionary Computation Conf.: Late Breaking Papers*, 1963–1966. New York: Association for Computing Machinery.

Asadzadeh, M., and B. A. Tolson. 2013. "Pareto archived dynamically dimensioned search with hypervolume-based selection for multi-objective optimization." *Eng. Optim.* 45 (12): 1489–1509. https://doi.org/10.1080/0305215X.2012.748046.

Bolouri-Yazdeli, Y., O. B. Haddad, E. Fallah-Mehdipour, and M. Mariño. 2014. "Evaluation of real-time operation rules in reservoir systems operation." *Water Resour. Manage.* 28 (3): 715–729. https://doi.org/10.1007/s11269-013-0510-1.

Boucher, M.-A., D. Tremblay, L. Delorme, L. Perreault, and F. Anctil. 2012. "Hydro-economic assessment of hydrological forecasting systems." *J. Hydrol.* 416 (Jan): 133–144. https://doi.org/10.1016/j.jhydrol.2011.11.042.

Buşoniu, L., D. Ernst, B. De Schutter, and R. Babuška. 2011. "Cross-entropy optimization of control policies with adaptive basis functions." *IEEE Trans. Syst. Man Cybern. Part B Cybern.* 41 (1): 196–209.

Chinese National Committee on Large Dams. 2011. *Ankang hydropower project*. Beijing: Chinese National Committee on Large Dams.

Cover, T. M. 1991. *Elements of information theory*, edited by T. M. Cover and J. A. Thomas. New York: Wiley.

Deisenroth, M. P., G. Neumann, and J. Peters. 2013. "A survey on policy search for robotics." *Found. Trends Rob.* 2 (1–2): 1–142. https://doi.org/10.1561/2300000021.

Denaro, S., D. Anghileri, M. Giuliani, and A. Castelletti. 2017. "Informing the operations of water reservoirs over multiple temporal scales by direct use of hydro-meteorological data." *Adv. Water Resour.* 103 (May): 51–63. https://doi.org/10.1016/j.advwatres.2017.02.012.

Faber, B. A., and J. Stedinger. 2001. "Reservoir optimization using sampling SDP with ensemble streamflow prediction (ESP) forecasts." *J. Hydrol.* 249 (1): 113–133. https://doi.org/10.1016/S0022-1694(01)00419-X.

Ficchì, A., L. Raso, D. Dorchies, F. Pianosi, P.-O. Malaterre, P.-J. Van Overloop, and M. Jay-Allemand. 2015. "Optimal operation of the multireservoir system in the Seine River Basin using deterministic and ensemble forecasts." *J. Water Resour. Plann. Manage.* 142 (1): 05015005. https://doi.org/10.1061/(ASCE)WR.1943-5452.0000571.

Funk, C., P. Peterson, M. Landsfeld, D. Pedreros, J. Verdin, S. Shukla, G. Husak, J. Rowland, L. Harrison, and A. Hoell. 2015. "The climate hazards infrared precipitation with stations—A new environmental record for monitoring extremes." *Sci. Data* 2 (1): 1–21. https://doi.org/10.1038/sdata.2015.66.

Georgakakos, A. 1989. "The value of streamflow forecasting in reservoir operation." *J. Am. Water Resour. Assoc.* 25 (4): 789–800. https://doi.org/10.1111/j.1752-1688.1989.tb05394.x.

Georgakakos, K., N. Graham, T. Carpenter, and H. Yao. 2005. "Integrating climate-hydrology forecasts and multi-objective reservoir management for northern California." *Eos Trans. Am. Geophys. Union* 86 (12): 122–127. https://doi.org/10.1029/2005EO120002.

Georgakakos, K. P., and N. E. Graham. 2008. "Potential benefits of seasonal inflow prediction uncertainty for reservoir release decisions." *J. Appl. Meteorol. Climatol.* 47 (5): 1297–1321. https://doi.org/10.1175/2007JAMC1671.1.

Gibbs, M. S., D. McInerney, G. Humphrey, M. A. Thyer, H. R. Maier, G. C. Dandy, and D. Kavetski. 2018. "State updating and calibration period selection to improve dynamic monthly streamflow forecasts for an environmental flow management application." *Hydrol. Earth Syst. Sci. Discuss.* 22: 871–887. https://doi.org/10.5194/hess-22-871-2018.

Giuliani, M., A. Castelletti, F. Pianosi, E. Mason, and P. M. Reed. 2015a. "Curses, tradeoffs, and scalable management: Advancing evolutionary multiobjective direct policy search to improve water reservoir operations." *J. Water Resour. Plann. Manage.* 142 (2): 04015050. https://doi.org/10.1061/(ASCE)WR.1943-5452.0000570.

Giuliani, M., E. Mason, A. Castelletti, F. Pianosi, and R. Soncini-Sessa. 2014. "Universal approximators for direct policy search in multi-purpose water reservoir management: A comparative analysis." *IFAC Proc. Volumes* 47 (3): 6234–6239. https://doi.org/10.3182/20140824-6-ZA-1003.01962.

Giuliani, M., F. Pianosi, and A. Castelletti. 2015b. "Making the most of data: An information selection and assessment framework to improve water systems operations." *Water Resour. Res.* 51 (11): 9073–9093. https://doi.org/10.1002/2015WR017044.

Gleick, P. H., and M. Palaniappan. 2010. "Peak water limits to freshwater withdrawal and use." *Proc. Natl. Acad. Sci.* 107 (25): 11155–11162. https://doi.org/10.1073/pnas.1004812107.

Huffman, G. J., D. T. Bolvin, E. J. Nelkin, D. B. Wolff, R. F. Adler, G. Gu, Y. Hong, K. P. Bowman, and E. F. Stocker. 2007. "The TRMM multisatellite precipitation analysis (TMPA): Quasi-global, multiyear, combined-sensor precipitation estimates at fine scales." *J. Hydrometeorol.* 8 (1): 38–55. https://doi.org/10.1175/JHM560.1.

Ismail, M. F., and W. Bogacki. 2017. "Scenario approach for the seasonal forecast of Kharif flows from Upper Indus Basin." *Hydrol. Earth Syst. Sci. Discuss.* 22 (2): 1391–1409. https://doi.org/10.5194/hess-22-1391-2018.

Knowles, J., and D. Corne. 1999. "The Pareto archived evolution strategy: A new baseline algorithm for Pareto multiobjective optimisation." In Vol. 1 of *Proc., Congress on Evolutionary Computation (CEC99)*, 98–105. Piscataway, NJ: IEEE.

Kullback, S., and R. A. Leibler. 1951. "On information and sufficiency." *Ann. Math. Stat.* 22 (1): 79–86. https://doi.org/10.1214/aoms/1177729694.

Labadie, J. W. 2004. "Optimal operation of multireservoir systems: State-of-the-art review." *J. Water Resour. Plann. Manage.* 130 (2): 93–111. https://doi.org/10.1061/(ASCE)0733-9496(2004)130:2(93).

Laio, F., and S. Tamea. 2007. "Verification tools for probabilistic forecasts of continuous hydrological variables." *Hydrol. Earth Syst. Sci. Discuss.* 11 (4): 1267–1277. https://doi.org/10.5194/hess-11-1267-2007.

Lamontagne, J., and J. Stedinger. 2018. "Generating synthetic streamflow forecasts with specified precision." *J. Water Resour. Plann. Manage.* 144 (4): 04018007. https://doi.org/10.1061/(ASCE)WR.1943-5452.0000915.

Li, S., W. Liu, S. Gu, X. Cheng, Z. Xu, and Q. Zhang. 2009. "Spatio-temporal dynamics of nutrients in the upper Han River basin, China." *J. Hazard. Mater.* 162 (2–3): 1340–1346. https://doi.org/10.1016/j.jhazmat.2008.06.059.

Lu, M., U. Lall, A. W. Robertson, and E. Cook. 2017. "Optimizing multiple reliable forward contracts for reservoir allocation using multitime scale streamflow forecasts." *Water Resour. Res.* 53 (3): 2035–2050. https://doi.org/10.1002/2016WR019552.

Maurer, E. P., and D. P. Lettenmaier. 2004. "Potential effects of long-lead hydrologic predictability on Missouri River main-stem reservoirs." *J. Clim.* 17 (1): 174–186. https://doi.org/10.1175/1520-0442(2004)017<0174:PEOLHP>2.0.CO;2.

Mortensen, E., S. Wu, M. Notaro, S. Vavrus, R. Montgomery, J. De Piérola, C. Sánchez, and P. Block. 2018. "Regression-based season-ahead drought prediction for southern Peru conditioned on large-scale climate variables." *Hydrol. Earth Syst. Sci.* 22 (1): 287–303. https://doi.org/10.5194/hess-22-287-2018.

Nash, J. 1970. "River flow forecasting through conceptual models, I: A discussion of principles." *J. Hydrol.* 10 (3): 398–409. https://doi.org/10.1016/0022-1694(70)90255-6.

Rani, D., and M. M. Moreira. 2010. "Simulation–optimization modeling: A survey and potential application in reservoir systems operation." *Water Resour. Manage.* 24 (6): 1107–1138. https://doi.org/10.1007/s11269-009-9488-0.

Rosenberg, E. A., A. W. Wood, and A. C. Steinemann. 2011. "Statistical applications of physically based hydrologic models to seasonal streamflow forecasts." *Water Resour. Res.* 47 (3): W00H14. https://doi.org/10.1029/2010WR010101.

Sankarasubramanian, A., U. Lall, F. A. Souza Filho, and A. Sharma. 2009. "Improved water allocation utilizing probabilistic climate forecasts: Short-term water contracts in a risk management framework." *Water Resour. Res.* 45 (11): W11409. https://doi.org/10.1029/2009WR007821.

Sene, K., W. Tych, and K. Beven. 2018. "Exploratory studies into seasonal flow forecasting potential for large lakes." *Hydrol. Earth Syst. Sci.* 22 (1): 127–141. https://doi.org/10.5194/hess-22-127-2018.

Stedinger, J. R., B. F. Sule, and D. P. Loucks. 1984. "Stochastic dynamic programming models for reservoir operation optimization." *Water Resour. Res.* 20 (11): 1499–1505. https://doi.org/10.1029/WR020i011p01499.

Stedinger, J. R., R. M. Vogel, S. U. Lee, and R. Batchelder. 2008. "Appraisal of the generalized likelihood uncertainty estimation (GLUE) method." *Water Resour. Res.* 44 (12): W00B06. https://doi.org/10.1029/2008WR006822.

Sun, X., C. Ma, and J. Lian. 2017. "Optimal operation of Danjiangkou reservoir using improved hedging model and considering the effects of historical decisions." *J. Water Resour. Plann. Manage.* 144 (1): 04017080. https://doi.org/10.1061/(ASCE)WR.1943-5452.0000868.

Tikk, D., L. T. Kóczy, and T. D. Gedeon. 2003. "A survey on universal approximation and its limits in soft computing techniques." *Int. J. Approximate Reasoning* 33 (2): 185–202. https://doi.org/10.1016/S0888-613X(03)00021-5.

Tolson, B. A., and C. A. Shoemaker. 2007. "Dynamically dimensioned search algorithm for computationally efficient watershed model calibration." *Water Resour. Res.* 43 (1): W01413. https://doi.org/10.1029/2005WR004723.

Turner, S. W., J. C. Bennett, D. E. Robertson, and S. Galelli. 2017. "Complex relationship between seasonal streamflow forecast skill and value in reservoir operations." *Hydrol. Earth Syst. Sci.* 21 (9): 4841. https://doi.org/10.5194/hess-21-4841-2017.

Voisin, N., A. F. Hamlet, L. P. Graham, D. W. Pierce, T. P. Barnett, and D. P. Lettenmaier. 2006. "The role of climate forecasts in western US power planning." *J. Appl. Meteorol. Climatol.* 45 (5): 653–673. https://doi.org/10.1175/JAM2361.1.

Wang, H., and J. Liu. 2013. "Reservoir operation incorporating hedging rules and operational inflow forecasts." *Water Resour. Manage.* 27 (5): 1427. https://doi.org/10.1007/s11269-012-0246-3.

Watkins, D. W., and W. Wei. 2008. "The value of seasonal climate forecasts and why water managers don't use them." In *Proc., World Environmental and Water Resources Congress 2008: Ahupua'A*, 316. Reston, VA: ASCE.

Xu, B., P. A. Zhong, Z. Stanko, Y. Zhao, and W. W. G. Yeh. 2015. "A multiobjective short-term optimal operation model for a cascade system of reservoirs considering the impact on long-term energy production." *Water Resour. Res.* 51 (5): 3353–3369. https://doi.org/10.1002/2014WR015964.

Yan, B., S. Guo, and L. Chen. 2014. "Estimation of reservoir flood control operation risks with considering inflow forecasting errors." *Stochastic Environ. Res. Risk Assess.* 28 (2): 359–368. https://doi.org/10.1007/s00477-013-0756-4.

Yang, G., S. Guo, P. Liu, L. Li, and Z. Liu. 2017a. "Multiobjective cascade reservoir operation rules and uncertainty analysis based on PA-DDS algorithm." *J. Water Resour. Plann. Manage.* 143 (7): 04017025. https://doi.org/10.1061/(ASCE)WR.1943-5452.0000773.

Yang, G., S. Guo, P. Liu, L. Li, and C. Xu. 2017b. "Multiobjective reservoir operating rules based on cascade reservoir input variable selection method." *Water Resour. Res.* 53 (4): 3446–3463. https://doi.org/10.1002/2016WR020301.

Yu, P.-S., T.-C. Yang, C.-M. Kuo, and Y.-T. Wang. 2014. "A stochastic approach for seasonal water-shortage probability forecasting based on seasonal weather outlook." *Water Resour. Manage.* 28 (12): 3905. https://doi.org/10.1007/s11269-014-0717-9.